Synthesis of oligonucleotides containing pyrazolo[3,4-*d*]-pyrimidines: The influence of 7-substituted 8-aza-7-deazaadenines on the duplex structure and stability

Frank Seela* and Matthias Zulauf

Laboratorium für Organische und Bioorganische Chemie, Institut für Chemie, Universität Osnabrück, Barbarastr. 7, D-49069 Osnabrück, Germany

Received (in Cambridge) 10th November 1998, Accepted 21st December 1998

The phosphoramidites **2a**–**d** derived from 7-bromo- (**1b**), 7-iodo- (**1c**), 7-(hex-1-ynyl)- (**1d**) and 7-(2-phenylethynyl)- (**1e**) 8-aza-7-deaza-2′-deoxyadenosine were prepared. They were employed in the solid-phase synthesis of various oligonucleotides containing the 8-aza-7-deazaadenine system instead of that of adenine. Their T_m-values were measured and their thermodynamic data were determined. The replacement of adenine residues by 8-aza-7-deazaadenine **1a** does not significantly influence the duplex stability, while the incorporation of 7-substituted derivatives **1b**–**e** led to much more stable duplexes compared with their adenine-containing counterparts. From the CD spectra of the oligonucleotide duplexes it is evident that the overall structure of a parent DNA is retained when only very few modified bases are incorporated. Structural changes do occur when the number of modified residues is increased. This might be the result of the high-*anti*-conformation of the 7-substituted 8-aza-7-deaza-2′-deoxyadenosine residues.

Introduction

The 7-substituents of 7-deazapurine (pyrrolo[2,3-*d*]pyrimidine; **A**) residues are well accommodated in the major groove of duplex DNA.[1–4] In general, these duplexes become stabilized by the modified nucleobases.[1–4] Thus, the 7-position of 7-deazapurines (purine numbering, **C**, is used throughout the Discussion section) can be used effectively for the functionalization of DNA with reporter groups of various types. Among the 7-deazapurine heterocycles the 8-aza-7-deazapurines (pyrazolo[3,4-*d*]pyrimidines; **B**) represent another isosteric purine system which can be functionalized at the same position by retaining the Watson–Crick recognition site of a "purine base".

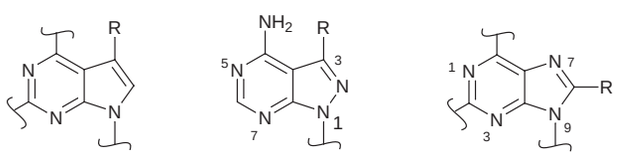

Structures of purine analogues.

The 8-aza-7-deazapurine nucleosides related to 2′-deoxyadenosine (dA) or 2′-deoxyguanosine (dG) have already been synthesized including those of the 7-halogenated or 7-alkynylated 8-aza-7-deaza-2′-deoxyadenosines.[5–9] Also 2′-deoxyribonucleosides carrying a 7-aminoalkyl group have been prepared.[10,11] Furthermore, 8-aza-7-deazapurine 2′-deoxyribonucleosides have been incorporated into oligonucleotides[12–19] and it was observed that the non-substituted 8-aza-7-deazaadenine-2′-deoxyriboside **1a** forms oligonucleotide duplexes with slightly enhanced stability compared with their adenine-containing counterparts.[13] Oligonucleotide duplexes containing 7-deazaadenine did not show this behaviour.[2,20]

As we wanted to combine the duplex-stabilizing effect of the 8-aza-7-deazapurine base with the favourable properties of the 7-substituents it was decided to incorporate compounds **1b**–**e** in oligonucleotides of various sequence patterns. For this purpose the building blocks **2a**–**d** were synthesized and used in solid-phase oligonucleotide synthesis. The oligonucleotides are studied with regard to their duplex structure and stability.

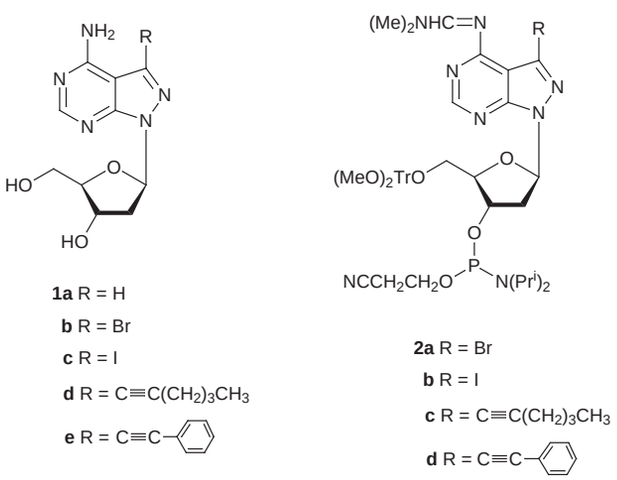

7-Substituted 8-aza-7-deazaadenine 2′-deoxyribofuranosides and phosphoramidite building blocks for the synthesis of oligonucleotides.

Results and discussion

Monomers

In a previous publication the synthesis of the 7-bromo-, 7-iodo- and 7-(2-phenylethynyl)-8-aza-7-deaza-2′-deoxyadenosines **1b**,**c**,**e** was described.[8] Following the cross-coupling protocol[8] and using compounds **1b** ($Br^7c^7z^8A_d$) or **1c** ($I^7c^7z^8A_d$) together with hex-1-yne the derivative **1d** ($Hxy^7c^7z^8A_d$) was synthesized (Scheme 1).

The 8-aza-7-deazaadenine nucleosides **1a**–**e** show CD spectra which are different from that of 2′-deoxyadenosine (dA) (Fig. 1). The latter shows a negative Cotton effect around

Table 1 Half-life-values ($t_{\frac{1}{2}}$) of deprotection of 8-aza-7-deazaadenine 2′-deoxyribonucleosides in 25% aq. NH_3 at 20 °C

Comp.	λ [nm]	$t_{\frac{1}{2}}$ [min]
fma^{6}Br^{7}c^{7}z^{8}A$_d$ **3a**	323	4
fma^{6}I^{7}c^{7}z^{8}A$_d$ **3b**	323	4 (120[a])
fma^{6}Hxy^{7}c^{7}z^{8}A$_d$ **3c**	321	10
fma^{6}Phy^{7}c^{7}z^{8}A$_d$ **3d**	319	12
bz^{6}I^{7}c^{7}z^{8}A$_d$ **4a**	314	145[b]
bu^{i6}I^{7}c^{7}z^{8}A$_d$ **4b**	299	71

[a] Measured in 10% aq. Na_2CO_3. [b] Measured at 60 °C.

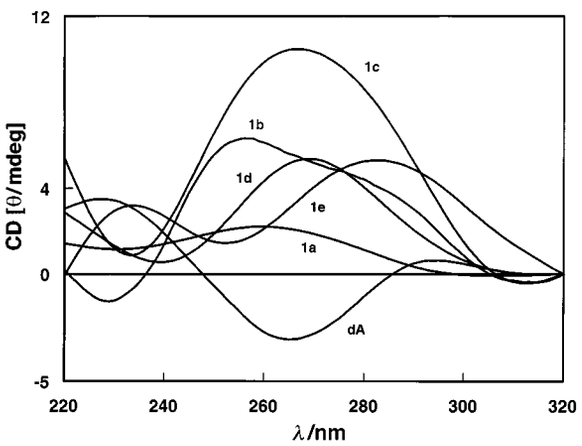

Fig. 1 CD spectra of nucleosides **1a**–**e** and dA, measured at 10 °C in 1 M NaCl, 100 mM $MgCl_2$ and 60 mM sodium cacodylate, $C_2H_6AsO_2NA$, (pH = 7.0) with 10 mM nucleoside concentration.

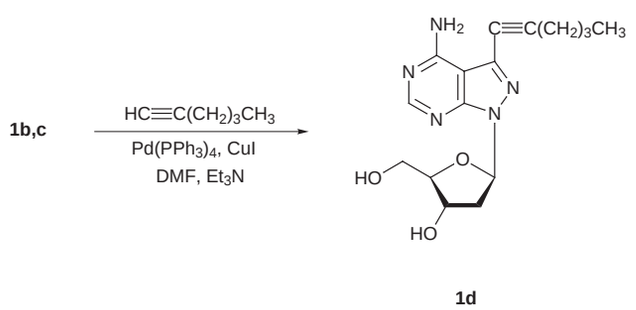

Scheme 1 Synthesis of 7-(hex-1-ynyl)-8-aza-7-deaza-2′-deoxyadenosine.

270 nm whereas the 8-aza-7-deaazaadenine nucleosides exhibit positive CD bands. Significant differences of the CD maxima are caused by the various 7-substituents. From X-ray studies of the related 8-azapurine nucleosides[21,22] it is known that these nucleosides possess a very particular conformation at the N-glycosylic bond, being different from that of 2′-deoxyadenosine. The conformational change of the N-glycosylic bond can also be found for compounds **1a**–**c**[23] which might cause a conformational change of the oligonucleotide structure—a phenomenon which is discussed later.

For the preparation of the oligonucleotide building blocks **2a**–**d** a selection of appropriate protecting groups was necessary. Two series of protecting groups, namely acyl and amidine residues, were studied (see structures **3** and **4**). The amidines **3a**–**d** were obtained from the reaction of free amines **1b**–**e** with dimethylformamide dimethyl acetal in MeOH. The benzoyl (Bz) and isobutyryl (COPr^i) derivatives **4a**,**b** were prepared from iodo amine **1c** using the acid chlorides and employing the protocol of transient protection.[24] The protecting-group stability was determined UV-spectrophotometrically in 25% aq. ammonia at 20 °C at the wavelength given in Table 1. From this table it is apparent that the acyl-

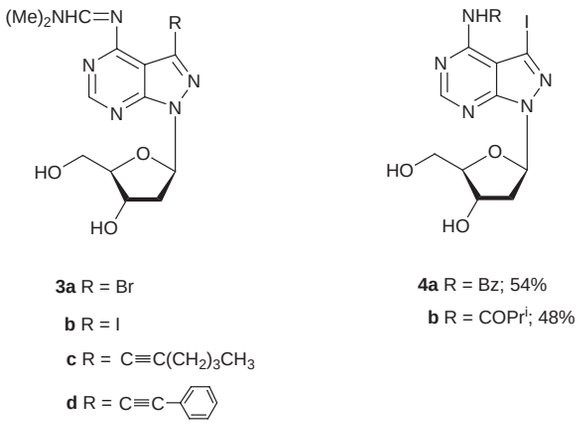

N^6-Amino-protected nucleosides.

ated compounds **4a**,**b** are more stable than the amidines **3a**–**d**. This observation is analogous to results obtained with the nucleoside **1a**.[13] Because of its ready introduction and the higher yields obtained, the formamidine residue was chosen. Subsequently, the 4,4′-dimethoxytriphenylmethyl group was introduced, yielding the 5′-protected nucleosides **5a**–**d** (Scheme 2). Phosphitylation with chloro(2-cyanoethoxy)(*N*,*N*-diiso-

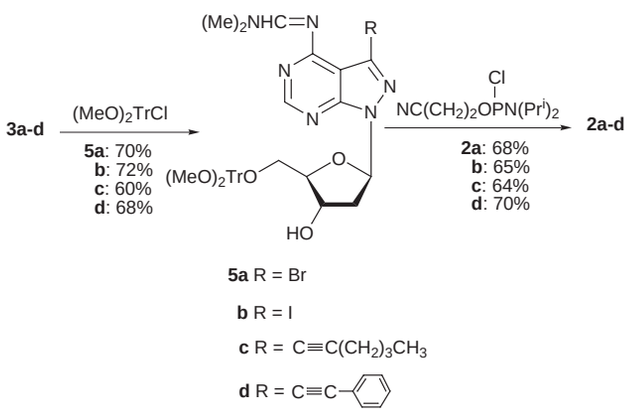

Scheme 2 Synthetic pathway to the 8-aza-7-deazaadenine nucleoside building blocks for DNA synthesis.

propylamino)phosphine in THF furnished the phosphoramidites **2a**–**d**.

All compounds were characterized by ^{1}H, ^{13}C and ^{31}P NMR spectra (Table 2 and Experimental section) as well as by elemental analyses. The assignment of the ^{13}C NMR signals of the derivatives **1d**, **3a**–**d**, **4a**,**b** and **5a**–**d** was made on the basis of gated-decoupled ^{13}C NMR spectra. From the NMR data of Table 2 a significant upfield shift of the C-7 signal can be seen for the halogenated compounds **1b**,**c**. The introduction of the amidine protecting group (⟶ **3a**–**d**) has a strong influence on the electronic properties of the base, which results in a significant downfield shift of the C-6 signals and changes of all other signals of the base. The 5′-OH-tritylation (⟶ **5a**–**d**) leads to an upfield shift of C-4′ and a downfield shift of C-5′.

Oligonucleotides

In order to study the influence of the 7-substituted 8-aza-7-deaza-2′-deoxyadenosine derivatives on the duplex stability of oligonucleotides, compounds **1a**–**e** were incorporated into oligomers having various sequence patterns and representing self-complementary and non-self-complementary oligonucleotides. Their synthesis was performed on a solid phase in an automated DNA synthesizer using the phosphoramidites **2a**–**d**, as well as that of 8-aza-7-deaza-2′-deoxyadenosine[13] and those of the regular DNA constituents. The oligonucleotides

Table 2 ^{13}C NMR chemical shifts of 8-aza-7-deazaadenine 2′-deoxyribofuranosides, measured in $(CD_3)_2SO$

a / *b*	C(7) / C(3)	C(5) / C(3a)	C(6) / C(4)	C(2) / C(6)	C(4) / C(7a)	(C1′)	(C2′)	C(3′)	C(4′)	C(5′)
1a	132.9	100.3	157.8	155.9	153.4	83.8	37.8	70.9	87.4	62.3
1b	118.9	99.8	157.3	156.9	154.5	84.0	37.8	70.8	87.7	62.3
1c	91.0	103.5	157.6	156.2	154.0	84.0	37.9	70.9	87.7	62.3
1d	127.5	100.7	157.1	155.7	153.3	84.0	37.9	70.9	87.8	62.5
1e	126.6	100.8	157.7	156.7	153.8	84.2	37.9	70.9	87.7	62.3
3a	120.9	106.1	161.8	156.1	155.0	84.0	37.8	70.8	87.6	62.3
3b	92.9	109.4	161.6	155.6	154.4	84.1	37.9	70.9	87.6	62.3
3c	129.0	107.7	162.2	155.7	154.4	83.9	37.7	70.9	87.6	62.3
3d	121.7	107.9	162.2	155.9	154.4	84.2	37.9	70.9	87.7	62.3
4a	94.4	112.0	154.6	155.5	154.2	84.2	37.8	70.8	87.9	62.2
4b	94.3	111.2	154.5	155.3	153.5	84.1	37.8	70.8	87.8	62.2
5a	121.0	106.2	161.8	156.2	155.0	83.8	38.0	70.6	85.4	64.2
5b	93.0	109.4	161.6	156.6	154.4	83.9	38.1	70.7	85.5	64.3
5c	128.9	107.8	162.2	155.7	154.4	83.7	37.9	70.6	85.3	64.1
5d	121.8	108.0	162.2	156.0	154.6	83.9	38.0	70.4	85.3	63.9

	C≡C	OMe	Me_2	HC=N	C=O
1d	96.9, 71.9				
1e	93.5, 80.7				
3a			34.9, 40.8	157.6	
3b			35.0, 40.7	157.3	
3c	73.4, 94.1		34.5, 40.7	157.6	
3d	82.3, 91.9		34.7, 40.7	157.7	
4a					176.8
4b			18.9, 19.4		176.3
5a		54.9	34.8, 40.7	157.5	
5b		54.9	35.0, 40.7	157.2	
5c	73.6, 93.8	54.9	34.5, 40.6	157.5	
5d	82.5, 91.8	54.8	34.7, 40.7	157.7	

[a] Purine numbering. [b] Systematic numbering.

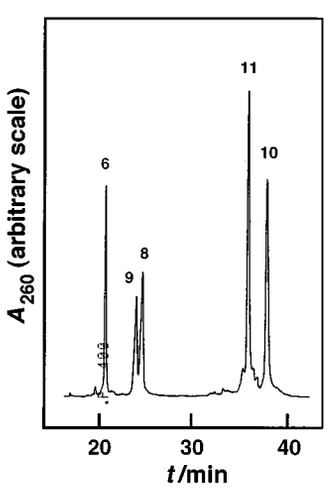

Fig. 2 HPLC profiles of the oligonucleotides 5′-d(A-T)$_6$ **6**, 5′-d(I^{7}c^{7}z^{8}A-T)$_6$ **8**, 5′-d(Br^{7}c^{7}z^{8}A-T)$_6$ **9**, 5′-d(Hxy^{7}c^{7}z^{8}A-T)$_6$ **10** and 5′-d(Phy^{7}c^{7}z^{8}A-T)$_6$ **11** after purification by reversed-phase (RP-18) chromatography, gradient *I*; for details see Experimental section.

were recovered, deprotected, and then purified using oligonucleotide-purification cartridges.[25] Their purity was checked by reversed-phase HPLC. According to Fig. 2 the retention time on the reversed-phase column is increased by the lipophilicity of the substituent. The nucleoside composition of the oligomers was established from reversed-phase HPLC profiles, obtained after hydrolysis with snake-venom phosphodiesterase followed by alkaline phosphatase. Also, MALDI-TOF mass spectra were measured in several cases (Table 3).

Self-complementary oligonucleotides with alternating bases or base tracts. Earlier investigations on oligonucleotides with modified bases have shown that self-complementary duplexes formed by alternating 5′-d(A-T)$_n$ are extraordinarily sensitive to base modification.[1,2] This results from the particular structure of these oligomers.[1,2] In order to study this behaviour oligonucleotides with the sequence 5′-d(A-T)$_6$ **6** were chosen. For comparison, another self-complementary sequence, namely 5′-d[(A)$_6$-(T)$_6$] **12**, was selected. The influence of the 7-substituents on the duplex stability was investigated on the basis of T_m-data (Table 4). Representative melting profiles are shown in Fig. 3. Surprisingly, the duplex **11·11** shows a weak hypochromicity, which leads to the assumption that another DNA structure is present.

For all duplexes, the thermodynamic data were determined by curve-shape analysis; in a few examples, also by the concentration dependence of the T_m-values. For the data calculation the program "Meltwin 3.0"[26] was used. Sufficient agreement of the thermodynamic data obtained by these two methods was observed for the duplexes of the oligomers **9** and **10**. This implies that no other species than single strands and duplexes are present in solution. These findings are in agreement with a two-state model of the melting process. The T_m-differences observed at high or low salt concentrations are also in line with an observation made earlier on duplexes containing 7-substituted 7-deazaadenines.[1]

Contrary to the findings discussed above, the T_m-value and thermodynamic data calculated for the duplex **11·11** carrying a planar aromatic residue differ significantly at high- *vs.* low-salt buffer. Also, the thermodynamic data calculated from curve-shape analysis or obtained from the concentration-dependent measurements are not comparable. This indicates that oligonucleotides with alternating bases carrying aromatic residues at position-7 form very particular structures different from those of the other 7-substituted duplexes. Probably, the phenyl residue is too bulky or competes with the stacking of the nucleobases.

The self-complementary duplexes 5′-d[(A)$_6$-(T)$_6$]$_2$ **12·12**, 5′-d[(I^{7}c^{7}z^{8}A)$_6$-(T)$_6$]$_2$ **14·14** and 5′-d[(Br^{7}c^{7}z^{8}A)$_6$-(T)$_6$]$_2$ **15·15**

Table 3 Relative molecular masses of oligonucleotides determined by MALDI-TOF mass spectra

	M^+ (Calc.) [Da]	M^+ (Found) [Da]
5′-d($I^7c^7z^8A$-T)$_6$ **8**	4397.8	4397.0
5′-d($Br^7c^7z^8A$-T)$_6$ **9**	4115.5	4114.2
5′-d[($I^7c^7z^8A_{11}$)-A] **37**	5081.4	5080.7
5′-d[($Br^7c^7z^8A_{11}$)-A] **38**	4564.4	4563.8
5′-d(CGCG($Hxy^7c^7z^8A$)$_2$TTCGCG) **20**	3806.7	3804.6
5′-d(CGCG($Phy^7c^7z^8A$)$_2$TTCGCG) **21**	3846.7	3884.3 $[M + K]^+$
5′-d(GT$Br^7c^7z^8$AG($Br^7c^7z^8A$)$_2$TTCT$Br^7c^7z^8$AC) **28**	3960.0	3959.6
5′-d(GT$Phy^7c^7z^8$AGAATTCTAC) **31**	3744.6	3743.9
5′-d(T$Hxy^7c^7z^8$AGGTCAAT$Hxy^7c^7z^8$ACT) **50**	3804.7	3806.3

Table 4 T_m-values and thermodynamic data of self-complementary oligonucleotides with alternating bases or base tracts of 7-halogeno- and 7-(alk-1-ynyl)-8-aza-7-deazaadenines[a]

Oligonucleotide	T_m [°C]	ΔH [kcal mol^{-1}][b]	ΔS [cal mol^{-1} K^{-1}][b]	ΔG^{298} [kcal mol^{-1}][b]
5′-d[(A-T)$_6$]$_2$ **6·6**	33(26)	−45(−44)	−125(−127)	−6.3(−5.5)
5′-d[(c^7z^8A-T)$_6$]$_2$ **7·7**[13]	36[13]			
5′-d[($I^7c^7z^8$A-T)$_6$]$_2$ **8·8**	56(52)	−61(−59)	−163(−160)	−10.5(−9.6)
5′-d[($Br^7c^7z^8$A-T)$_6$]$_2$ **9·9**	52(49)	−59(−50)	−157(−133)	−9.7(−8.6)
		−66[c]	−180[c]	−10.0[c]
5′-d[($Hxy^7c^7z^8$A-T)$_6$]$_2$ **10·10**	56(51)	−61(−53)	−163(−142)	−10.6(−9.4)
		−58[c]	−154[c]	−10.4[c]
5′-d[($Phy^7c^7z^8$A-T)$_6$]$_2$ **11·11**	56(31)	−59(−32)	−157(−83)	−10.3(−6.1)
		−16[c]	−28[c]	−8.0[c]
5′-d[(A)$_6$-(T)$_6$]$_2$ **12·12**	46(40)	−81(−75)	−232(−219)	−9.1(−7.4)
5′-d[(c^7z^8A)$_6$-(T)$_6$]$_2$ **13·13**	44(39)	−49(−58)	−133(−163)	−8.3(−7.1)
5′-d[($I^7c^7z^8$A)$_6$-(T)$_6$]$_2$ **14·14**	71(66)	−108(−78)	−291(−207)	−17.4(−13.7)
5′-d[($Br^7c^7z^8$A)$_6$-(T)$_6$]$_2$ **15·15**	62(60)	−99(−80)	−272(−240)	−14.2(−13.2)
		−114[c]	−318[c]	−15.3[c]

[a] Determined at 270 nm. Data without parentheses are measured in 1 M NaCl containing 100 mM $MgCl_2$ and 60 mM sodium cacodylate (pH = 7.0) with 10 μM oligonucleotide concentration. Data in parentheses are measured in 0.1 M NaCl, 10 mM $MgCl_2$ and 10 mM sodium cacodylate (pH = 7.0) with 10 μM oligonucleotide concentration. [b] 1 cal = 4.184 J. [c] Determined from the concentration dependence of the T_m-values.

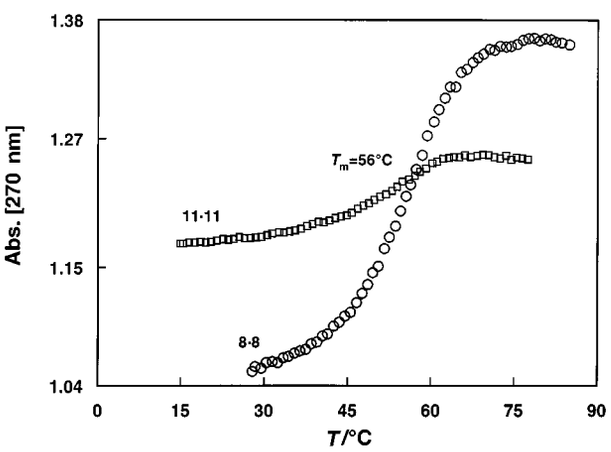

Fig. 3 Melting profiles of the alternating duplexes 5′-d[($I^7c^7z^8$A-T)$_6$]$_2$ **8·8** and 5′-d[($Phy^7c^7z^8$A-T)$_6$]$_2$ **11·11**, measured at 270 nm in 1 M NaCl, 100 mM $MgCl_2$ and 60 mM sodium cacodylate (pH = 7.0) with 10 μM oligomer concentration.

(Table 4) containing tracts of dA and dT have the same number of base pairs as the alternating compounds derived from 5′-d[(A-T)$_6$]$_2$ **6·6**. According to nearest-neighbour influence the T_m-values of the alternating duplexes compared with those with runs of dA or dT differ significantly from each other. Nevertheless, the tendency of duplex stabilization found for the alternating oligomers is similar to that for those oligomers containing alternating dA-dT. The T_m-increase per modified dA-dT base pair is 4.2 °C in the case of the iodo-containing duplex **14·14** and 2.7 °C for the bromo-containing duplex **15·15**. For comparison, the T_m-increase for one base pair of the alternating duplexes is 3.8 °C in the case the duplex **8·8** and 3.2 °C for the hybrid **9·9**.

The CD spectra of the alternating oligonucleotide duplexes containing 8-aza-7-deazaadenine, *e.g.* **8·8**, **9·9** and **10·10**, show similarities to that of the parent duplex 5′-d[(A-T)$_6$]$_2$ **6·6** (Fig. 4). However, the positive as well as the negative CD maxima are shifted bathochromically. The duplex **11·11** with a phenylethynyl moiety at the 7-position shows a positive Cotton effect at 300 nm and two negative Cotton effects at 253 nm and 280 nm (Fig. 5a). At elevated temperature a main maximum can be observed at 283 nm. Contrary to other duplexes, the CD spectra in the low-salt buffer are remarkably different from that in the high-salt medium (Fig. 5b).

Significant changes occur in the CD spectra of duplexes derived from the sequence 5′-d[(A)$_6$-(T)$_6$] **12**. In particular, the duplex **14·14** with 7-iodo substituents differs from the others (Fig. 6).

Self-complementary palindromic oligonucleotides. Apart from the studies on alternating self-complementary oligonucleotides the 7-substituted 8-aza-7-deazaadenine residues were incorporated in palindromic oligonucleotides. The investigations were performed on the Dickerson–Drew duplex 5′-d(CGCGAATTCGCG)[27] **16** and the related compound 5′-d(GTAGAATTCTAC) **22**, both containing the recognition site of the endodeoxyribonuclease Eco RI [5′-d(GAATTC)].[28] The replacement of dA-residues by the 7-substituted 8-aza-7-deaza-2′-deoxyadenosines **1b–d** enhances the duplex stability compared with the parent duplexes **16·16** and **22·22** (Table 5). The higher the substitution grade, the more the stability increases. The 7-halogeno as well as the 7-alkynyl substituents increase the duplex stability significantly in both series of compounds. The duplex stability was not significantly altered

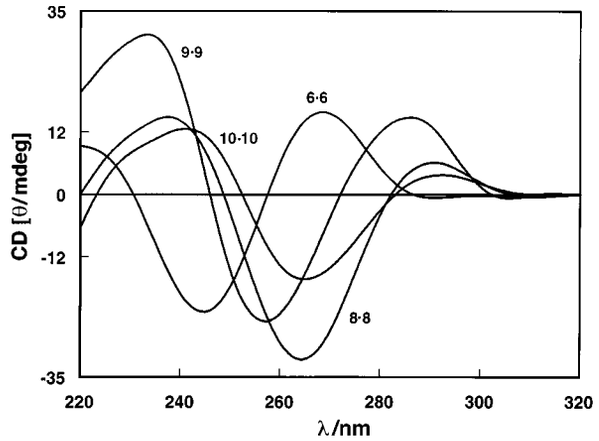

Fig. 4 CD spectra of the alternating duplexes 5′-d[(A-T)$_6$]$_2$ **6·6**, 5′-d[(I^{7}c^{7}z^{8}A-T)$_6$]$_2$ **8·8**, 5′-d[(Br^{7}c^{7}z^{8}A-T)$_6$]$_2$ **9·9** and 5′-d[(Hxy^{7}c^{7}z^{8}A-T)$_6$]$_2$ **10·10**, measured at 10 °C in 1 M NaCl, 100 mM $MgCl_2$ and 60 mM sodium cacodylate (pH = 7.0) with 10 μM oligomer concentration.

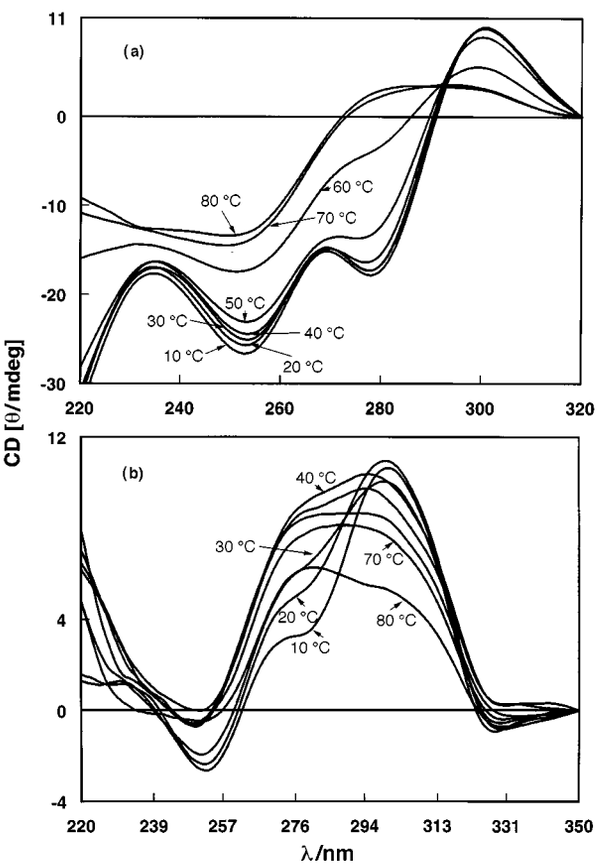

Fig. 5 CD spectra of the alternating duplex 5′-d[(Phy^{7}c^{7}z^{8}A-T)$_6$]$_2$ **11·11**, measured between 10–80 °C in (a) 1 M NaCl, 100 mM $MgCl_2$ and 60 mM sodium cacodylate (pH = 7.0) with 10 μM oligomer concentration and (b) 0.1 M NaCl, 10 mM $MgCl_2$ and 10 mM sodium cacodylate (pH = 7.0) with 10 μM oligomer concentration.

when c^{7}z^{8}A$_d$ **1a** replaces dA (duplexes **17·17**, **23·23** and **24·24**). Surprisingly, the modified Dickerson–Drew duplex 5′-d[(CGCG(Phy^{7}c^{7}z^{8}A)$_2$TTCGCG)]$_2$ **21·21** exhibits a rather low stability. The other sequences containing the planar 7-phenylethynyl residue show a slightly increased stability (compounds **30·30** and **31·31**). As palindromic duplexes show a tendency to form hairpin structures, in particular at low salt concentration in the absence of Mg^{2+},[29] T_m-measurements were performed in 1 M or 0.1 M NaCl in the presence of $MgCl_2$. The acceptable agreement of the thermodynamic data obtained by shape analysis of the melting curves and from the concentration dependence of the T_m-values (Table 5, Fig. 7) indicates that a duplex melting has taken place.

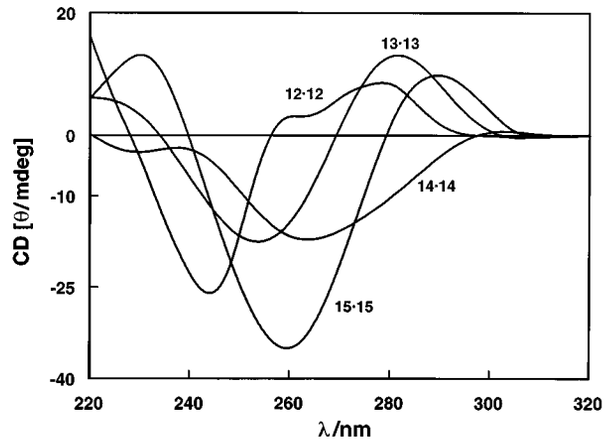

Fig. 6 CD spectra of the block oligonucleotide duplexes 5′-d[(A)$_6$-(T)$_6$]$_2$ **12·12**, 5′-d[(c^{7}z^{8}A)$_6$-(T)$_6$]$_2$ **13·13**, 5′-d[(I^{7}c^{7}z^{8}A)$_6$-(T)$_6$]$_2$ **14·14** and 5′-d[(Br^{7}c^{7}z^{8}A)$_6$-(T)$_6$]$_2$ **15·15**, measured at 10 °C in 1 M NaCl, 100 mM $MgCl_2$ and 60 mM sodium cacodylate (pH = 7.0) with 10 μM oligomer concentration.

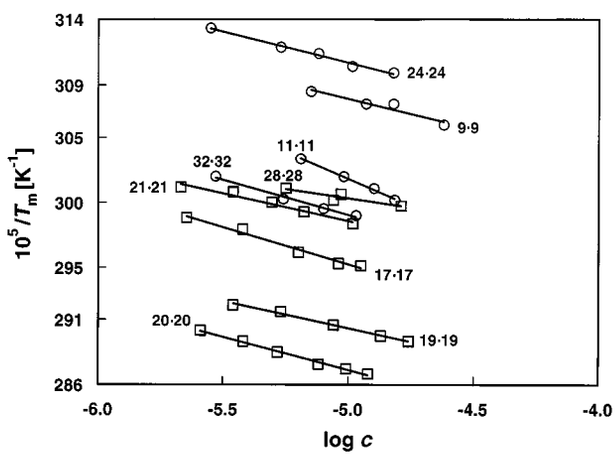

Fig. 7 $1/T_m$ *vs.* log *c* plot of palindromic Dickerson–Drew duplexes **17·17**, **19·19**, **20·20** and **21·21** and of the alternating or self-complementary duplexes **9·9**, **11·11**, **24·24**, **28·28** and **32·32**; for sequences see Tables 4 and 5.

Homooligonucleotides. For this investigation the oligonucleotide "homomers" **33** and **35**–**39** were synthesized and hybridized with d(T)$_{12}$ **34**. According to Table 6 a slight duplex destabilization occurs when the dA-residues of d(A)$_{12}$ **33** are replaced by c^{7}z^{8}A$_d$ **1a** (⟶ **34·35**). This decrease is less pronounced when the number of modified bases is reduced and c^{7}z^{8}A$_d$ **1a** alternates with dA (duplex **34·36**). However, when the duplexes contain 8-aza-7-deazaadenine residues carrying 7-bromo, 7-iodo or 7-hexynyl substituents (compounds **1b**–**d**) a much higher stability is observed. The duplex formed by the iodo-containing homomer **37** with d(T)$_{12}$ **34** shows the highest T_m-value. Earlier, T_m-values were determined from the same type of d(A$_{12}$)·d(T$_{12}$) duplex but containing 7-deazaadenine or 7-substituted 7-deazaadenine residues instead of adenine.[1,2] In this case the T_m-decrease of the duplex with the unsubstituted 7-deazaadenine (4-aminopyrrolo[2,3-*d*]pyrimidine) base was much stronger than that observed for the unsubstituted 8-aza-7-deazaadenine (4-aminopyrazolo[3,4-*d*]pyrimidine). Also the T_m-increase induced by the 7-substituents was not as strong as found for the 7-substituted compounds of Table 6.

Base-stacking interactions within single-stranded oligonucleotides can be stronger than in oligonucleotide duplexes.[30] This can lead to highly organized single-stranded helices. The preorganization of such a single strand influences the duplex in such a way that the more stable secondary structure of one single strand determines the secondary structure of the

Table 5 T_m-values and thermodynamic data of self-complementary oligonucleotides containing 7-halogeno- and 7-(alk-1-ynyl)-8-aza-7-deazaadenines[a]

Oligonucleotide	T_m [°C]	ΔH [kcal mol^{-1}][b]	ΔS [cal mol^{-1} K^{-1}][b]	ΔG^{298} [kcal mol^{-1}][b]
5′-d[(CGCGAATTCGCG)]$_2$ **16·16**	64(63)	−83(−73)	−224(−195)	−13.7(−12.6)
5′-d[(CGCG(c^{7}z^{8}A)$_2$TTCGCG)]$_2$ **17·17**	64(63)	−84(−72)	−226(−193)	−13.7(−12.5)
		(−72)[c]	(−190)[c]	(−12.7)[c]
5′-d[(CGCG(I^{7}c^{7}z^{8}A)$_2$TTCGCG)]$_2$ **18·18**	72(71)	−101(−93)	−272(−247)	−17.0(−16.0)
5′-d[(CGCG(Br^{7}c^{7}z^{8}A)$_2$TTCGCG)]$_2$ **19·19**	71(69)	−99(−95)	−266(−255)	−16.5(−16.0)
		−104[c]	−279[c]	−17.0[c]
5′-d[(CGCG(Hxy^{7}c^{7}z^{8}A)$_2$TTCGCG)]$_2$ **20·20**	75(74)	−87(−96)	−227(−254)	−16.2(−17.4)
		−92[c]	−244[c]	−16.9[c]
5′-d[(CGCG(Phy^{7}c^{7}z^{8}A)$_2$TTCGCG)]$_2$ **21·21**	62(61)	−51(−47)	−130(−117)	−10.8(−10.7)
		−69[c]	−183[c]	−12.2[c]
5′-d[(GTAGAATTCTAC)]$_2$ **22·22**	46(43)	−79(−84)	−226(−225)	−9.2(−8.6)
5′-d[(GTc^{7}z^{8}AGAATTCTc^{7}z^{8}AC)]$_2$ **23·23**	47(44)	−60(−65)	−166(−183)	−8.8(−8.2)
5′-d[(GTc^{7}z^{8}AG(c^{7}z^{8}A)$_2$TTCTc^{7}z^{8}AC)]$_2$ **24·24**	48(44)	−77(−75)	−216(−213)	−9.6(−8.6)
		−82[c]	−235[c]	−9.8[c]
5′-d[(GTAG(I^{7}z^{8}A)$_2$TTCTAC)]$_2$ **25·25**	54(52)	−87(−79)	−244(−219)	−11.6(−10.0)
5′-d[(GTAGI^{7}c^{7}z^{8}AATTCTAC)]$_2$ **26·26**	50	−86	−243	−10.3
5′-d[(GTI^{7}c^{7}z^{8}AGAATTCTAC)]$_2$ **27·27**	50	−83	−235	−10.2
5′-d[(GTBr^{7}c^{7}z^{8}AG(Br^{7}c^{7}z^{8}A)$_2$TTCTBr^{7}c^{7}z^{8}AC)]$_2$ **28·28**	60(56)	−61(−60)	−163(−160)	−11.1(−10.7)
		−63[c]	−166[c]	−11.1[c]
5′-d[(GTAG(Br^{7}c^{7}z^{8}A)$_2$TTCTAC)]$_2$ **29·29**	55(53)	−83(−88)	−232(−250)	−11.5(−10.9)
		−78[c]	−215[c]	−11.3[c]
5′-d[(GTAGPhy^{7}c^{7}z^{8}AATTCTAC)]$_2$ **30·30**	48	−78	−221	−9.6
		−87[c]	−250[c]	−9.9[c]
5′-d[(GTPhy^{7}c^{7}z^{8}AGAATTCTAC)]$_2$ **31·31**	48	−68	−191	−9.1
		−79[c]	−225[c]	−9.4[c]
5′-d[(GTHxy^{7}c^{7}z^{8}AG(Hxy^{7}c^{7}z^{8}A)$_2$TTCTHxy^{7}c^{7}z^{8}AC)]$_2$ **32·32**	60(55)	−84(−76)	−230(−210)	−13.0(−11.1)
		−81[c]	−220[c]	−12.7[c]

[a] Determined at 270 nm. Data without parentheses are measured in 1 M NaCl containing 100 mM $MgCl_2$ and 60 mM sodium cacodylate (pH = 7.0) with 10 μM oligonucleotide concentration. Data in parentheses are measured in 0.1 M NaCl, 10 mM $MgCl_2$ and 10 mM sodium cacodylate (pH = 7.0) with 10 μM oligonucleotide concentration. [b] 1 cal = 4.184 J. [c] Determined from the concentration dependence of the T_m-values.

Table 6 T_m-values and thermodynamic data of non-self-complementary oligonucleotides containing consecutive base residues of 7-halogeno- and 7-(alk-1-ynyl)-8-aza-7-deazaadenines[a]

Oligonucleotide	T_m [°C]	ΔH [kcal mol^{-1}][b]	ΔS [cal mol^{-1} K^{-1}][b]	ΔG^{298} [kcal mol^{-1}][b]
d(A)$_{12}$·d(T)$_{12}$ **33·34**	44(37)	−84(−91)	−238(−267)	−9.8(−7.9)
5′-d[(c^{7}z^{8}A)$_{11}$-A]·d(T)$_{12}$ **35·34**	38(32)	−91(−65)	−266(−186)	−8.4(−6.8)
5′-d[(c^{7}z^{8}A-A)$_6$]·d(T)$_{12}$ **36·34**	42(36)	−78(−80)	−222(−234)	−9.4(−7.7)
5′-d[(I^{7}c^{7}z^{8}A)$_{11}$-A]·d(T)$_{12}$ **37·34**	65(63)	−102(−90)	−276(−240)	−16.0(−15.0)
5′-d[(Br^{7}c^{7}z^{8}A)$_{11}$-A]·d(T)$_{12}$ **38·34**	63(58)	−87(−89)	−234(−242)	−14.4(−13.3)
5′-d(Hxy^{7}c^{7}z^{8}A-A)$_6$·d(T)$_{12}$ **39·34**	50	−82	−230	−10.8

[a] Determined at 270 nm. Data without parentheses are measured in 1 M NaCl containing 100 mM $MgCl_2$ and 60 mM sodium cacodylate (pH = 7.0) with 10 μM oligonucleotide concentration. Data in parentheses are measured in 0.1 M NaCl, 10 mM $MgCl_2$ and 10 mM sodium cacodylate (pH = 7.0) with 10 μM oligonucleotide concentration. [b] 1 cal = 4.184 J.

duplex. As the CD spectra give information on the secondary structure of single-stranded oligomers the CD spectra of 5′-d[(c^{7}z^{8}A)$_{11}$-A] **35**, 5′-d[(I^{7}c^{7}z^{8}A)$_{11}$-A] **37**, 5′-d[(Br^{7}c^{7}z^{8}A)$_{11}$-A] **38** and 5′d[(Hxy^{7}c^{7}z^{8}A-A)$_6$] **39** were measured. According to Fig. 8 the CD spectra of the non-substituted 5′-d[(c^{7}z^{8}A)$_{11}$-A] **35** looks similar to that of d(A)$_{12}$ **33**. Significant changes occur when the oligonucleotides carry 7-bromo or 7-iodo substituents. The CD spectra imply that the halogenated oligonucleotides have a more rigid structure than do their non-substituted counterparts.

When the CD spectra of the hybrids formed by the homomers **35**–**39** and d(T$_{12}$) **34** (Fig. 9) are compared with those of the pure homomers it is apparent that rather small changes of the CD spectra take place. The major change is a hypsochromic shift of the CD bands of the duplexes compared to the "purine" single strands. In the case of the regular d(A$_{12}$)·d(T$_{12}$) **33·34** duplex this shift is not observed, instead an extra CD band around 260 nm appears. According to these observations we suggest that the duplexes adopt the secondary structure of the "purine" single strands.

Oligonucleotides with random base composition. The oligonucleotides discussed above follow special sequences and are not representative of natural DNA. Therefore, another duplex was chosen. The duplexes 5′-d(TAGGTCAATACT) **40** and 3′-d(ATCCAGTTATGA) **41** are used as standard duplexes in our laboratory. Many base modifications have been studied on this hybrid. When 8-aza-7-deazaadenines replace adenine, the stability of duplexes stays unchanged (compounds **42·43** and **42·44**). In the cases when the 7-substituted 8-aza-7-deazaadenine residues replace adenine moieties a duplex stabilization was observed. This stabilization amounts to 1.5–1.8 °C per modified dA residue. Apart from this, the oligodeoxyribonucleotides **45** and **51** were hybridized with the oligoribonucleotide **52**. These RNA/DNA duplexes are less stable than those formed by two DNA strands (duplexes **45·52** and **51·52**)—an observation which has been made in other cases.[31] The stabilization by the 7-halogeno or 7-hexynyl substituents is also substantial in all cases displayed in Table 7. Again, the stability increase induced by the 8-aza-7-deazaadenine residues is more striking than for the type of duplexes containing

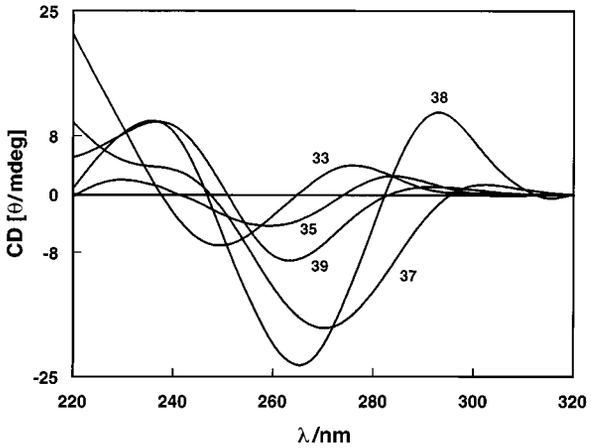

Fig. 8 CD spectra of the single-stranded homooligonucleotides $d(A)_{12}$ **33**, 5′-d[$(c^7z^8A)_{11}$-A] **35**, 5′-d[$(I^7c^7z^8A)_{11}$-A] **37**, 5′d[$(Br^7c^7z^8A)_{11}$-A] **38** and 5′-d$(Hxy^7c^7z^8A\text{-}A)_6$ **39**, measured at 10 °C in 1 M NaCl, 100 mM $MgCl_2$ and 60 mM sodium cacodylate (pH = 7.0) with 10 μM oligomer concentration.

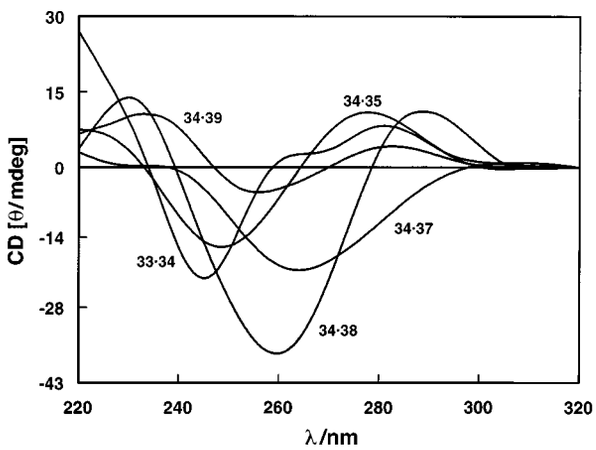

Fig. 9 CD spectra of the heteroduplexes $d(A)_{12}$·$d(T)_{12}$ **33·34**, 5′-d[$(c^7z^8A)_{11}$-A]·$d(T)_{12}$ **35·34**, 5′-d[$(I^7c^7z^8A)_{11}$-A]·$d(T)_{12}$ **37·34**, 5′-d[$(Br^7c^7z^8A)_{11}$-A]·$d(T)_{12}$ **38·34** and 5′-d$(Hxy^7c^7z^8A\text{-}A)_6$·$d(T)_{12}$ **39·34**, measured at 10 °C in 1 M NaCl, 100 mM $MgCl_2$ and 60 mM sodium cacodylate (pH = 7.0) with 10 μM oligomer concentration.

7-deazaadenines.[1] The oligodeoxyribonucleotide duplexes containing 7-substituted 8-aza-7-deazaadenines show the spectrum of a B-like DNA (Fig. 10). The DNA/RNA hybrids **45·52** and **51·52** adopt an A-like structure.

Conclusions and outlook

The most striking feature of oligonucleotides containing 7-substituted 8-aza-7-deazaadenines is their increased duplex stability over those containing the purine base adenine. This stabilizing effect is much stronger than in the case of the 7-substituted 7-deazaadenines.[1,2] As expected, the increase of the T_m-value depends on the number of modified bases and their sequence. It can reach up to 4.2 °C per modified d(A*-T) base pair. Steric constraints induced by the 8-substituents of purines or the 6-position of pyrimidines are not observed.[32–35] With regard to duplex stability the non-substituted 8-aza-7-deazaadenine behaves similarly to the parent adenine. The thermodynamic data of duplex melting which have been calculated by curve-shape analysis and in a few cases by the concentration dependence of the T_m-values are too crude to allow a detailed discussion on the contribution of enthalpic or entropic changes of duplex melting. Nevertheless, enthalpic changes seem to play the major part in duplex stabilization.

Inspection of the CD data of the various oligonucleotide single strands and duplexes and their comparison with those

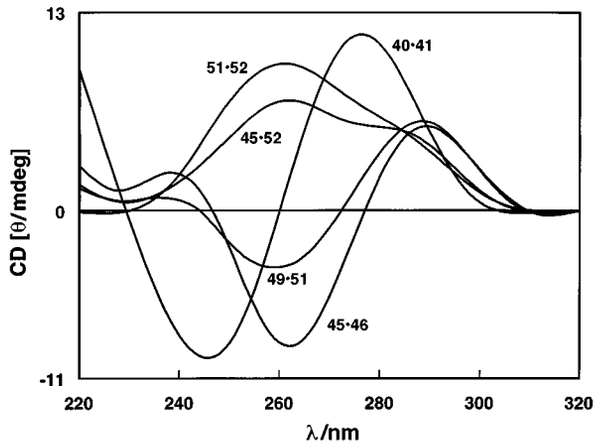

Fig. 10 CD spectra of the heteroduplexes **40·41**, **45·46**, **49·51**, **45·52** and **51·52**, measured at 10 °C in 1 M NaCl, 100 mM $MgCl_2$ and 60 mM sodium cacodylate (pH = 7.0) with 10 μM oligomer concentration; for sequences see Table 7.

for the parent adenine-containing compounds show that the secondary structure of the base-modified oligonucleotides may be altered. The effect is most striking when the oligonucleotide contains many 7-substituted 8-aza-7-deazaadenines. Duplexes with a random composition and only very few 8-aza-7-deazaadenine (4-aminopyrazolo[3,4-*d*]pyrimidine) residues adopt the overall B-DNA structure of the parent purine oligomer. The change from a B-DNA to an A-type structure is observed when the base-modified oligodeoxyribonucleotide is hybridized with an oligoribonucleotide.

According to X-ray analyses performed on compounds **1a–c** the conformation of the nucleosides around the N-glycosylic bonds is high-*anti* (**1a**: $\chi^1 = -106°$, **1b**: $\chi^1 = -75°$, **1c**: $\chi^1 = -73°$)[27] and not *anti* as found for 2′-deoxyadenosine ($\chi^1 = -165°$).[36] The influence of the 7-substitutents should be noticed (dA→**1a**→**1b**→**1c**).

This conformational change can influence the secondary structure of an oligonucleotide. According to a model for nucleosides with high-*anti*-conformation a vertical stacking of bases within an oligonucleotide duplex has been proposed.[37,38] The difference between this spatial arrangement and that of the familiar Watson–Crick duplex is a horizontally stabilized structure compared with the vertically stabilized Watson–Crick duplex. Apart from these structural considerations it is obvious that the incorporation of 7-substituted 7-deaza-8-azapurine residues enhances the stability of DNA and DNA/RNA duplexes. Furthermore, as in the case of 7-deaazapurines (pyrrolo[2,3-*d*]-pyrimidines) the 7-position accommodates rather bulky reporter groups useful for the labelling of DNA or RNA.

Experimental

General

Monomers. Chemicals were supplied by Aldrich, Sigma or Fluka. Solvents were of laboratory grade, except those used for HPLC, which were of HPLC grade. CHN analyses were performed by Mikroanalytisches Labor Beller (Göttingen, Germany). NMR Spectra were measured on AC 250 or AMX 500 spectrometers (Bruker, Germany) operating at proton resonance frequencies of 250.13 MHz and 500.14 MHz (125.13 MHz for ^{13}C and 101.3 MHz for ^{31}P), respectively. Chemical shifts are in ppm relative to TMS as internal standard or external 85% H_3PO_4. *J*-Values are given in Hz. Mps were measured with a Büchi SMP-20 apparatus (Büchi, Switzerland) and are uncorrected. UV spectra were recorded on a U 3200 spectrometer (Hitachi, Japan). TLC was performed on aluminium sheets, silica gel 60 F_{254}, 0.2 mm layer (Merck, Germany), and column chromatography (flash chromatography: FC) on silica gel 60 (Merck, Germany) at 0.4 bar

Table 7 T_m-values and thermodynamic data of non-self-complementary oligonucleotide duplexes containing 7-halogeno- and 7-(alk-1-ynyl)-8-aza-7-deazaadenines[a]

Oligonucleotide	T_m [°C]	ΔH [kcal mol^{-1}][b]	ΔS [cal mol^{-1} K^{-1}][b]	ΔG^{298} [kcal mol^{-1}][b]
5′-d(TAGGTCAATACT) **40** 3′-d(ATCCAGTTATGA) **41**	50(47)	−90(−82)	−252(−230)	−11.8(−10.4)
3′-d(ATCCc^{7}z^{8}AGTTc^{7}z^{8}ATGA) **42** 5′-d(Tc^{7}z^{8}AGGTCAATc^{7}z^{8}ACT) **43**	50(47)	−93(−90)	−261(−257)	−11.9(−11.0)
3′-d(ATCCc^{7}z^{8}AGTTc^{7}z^{8}ATGA) **42** 5′-d(Tc^{7}z^{8}AGGTC(c^{7}z^{8}A)$_2$Tc^{7}z^{8}ACT) **44**	50(47)	−88(−97)	−247(−260)	−11.5(−10.9)
5′-d(TI^{7}c^{7}z^{8}AGGTC(I^{7}c^{7}z^{8}A)$_2$TI^{7}c^{7}z^{8}ACT) **45** 3′-d(ATCCI^{7}c^{7}z^{8}AGTTI^{7}c^{7}z^{8}ATGA) **46**	61(58)	−95(−95)	−259(−261)	−14.8(−13.9)
5′-d(TI^{7}c^{7}z^{8}AGGTC(I^{7}c^{7}z^{8}A)$_2$TI^{7}c^{7}z^{8}ACT) **45** 3′-d(ATCCAGTTATGA) **41**	56(53)	−89(−93)	−245(−258)	−13.4(−12.8)
5′-d(TBr^{7}c^{7}z^{8}AGGTC(Br^{7}c^{7}z^{8}A)$_2$TBr^{7}c^{7}z^{8}ACT) **47** 3′-d(ATCCBr^{7}c^{7}z^{8}AGTTBr^{7}c^{7}z^{8}ATGA) **48**	61(57)	(−111)	(−308)	(−15.2)
5′-d(TBr^{7}c^{7}z^{8}AGGTC(Br^{7}c^{7}z^{8}A)$_2$TBr^{7}c^{7}z^{8}ACT) **47** 3′-d(ATCCAGTTATGA) **41**	56(52)	−83(−87)	−227(−242)	−12.7(−12.3)
5′-d(TAGGTCAATACT) **40** 3′-d(ATCCBr^{7}c^{7}z^{8}AGTTBr^{7}c^{7}z^{8}ATGA) **48**	55(51)	−81	−222	−12.7
3′-d(ATCCHxy^{7}c^{7}z^{8}AGTTHxy^{7}c^{7}z^{8}ATGA) **49** 5′-d(THxy^{7}c^{7}z^{8}AGGTCAATHxy^{7}c^{7}z^{8}ACT) **50**	57(53)	−90(−93)	−247(−261)	−13.4(−12.4)
3′-d(ATCCHxy^{7}c^{7}z^{8}AGTTHxy^{7}c^{7}z^{8}ATGA) **49** 5′-d(THxy^{7}c^{7}z^{8}AGGTC(Hxy^{7}c^{7}z^{8}A)$_2$THxy^{7}c^{7}z^{8}ACT) **51**	62(58)	−95(−86)	−259(−235)	−15.0(−13.4)
5′-d(TAGGTCAATACT) **40** 3′-r(AUCCAGUUAUGA) **52**	48(46)	−65(−82)	−176(−230)	−10.2(−10.1)
5′-d(TI^{7}c^{7}z^{8}AGGTC(I^{7}c^{7}z^{8}A)$_2$TI^{7}c^{7}z^{8}ACT) **45** 3′-r(AUCCAGUUAUGA) **52**	49	−87	−246	−11.0
3′-r(AUCCAGUUAUGA) **52** 5′-d(THxy^{7}c^{7}z^{8}AGGTC(Hxy^{7}c^{7}z^{8}A)$_2$THxy^{7}c^{7}z^{8}ACT) **51**	48	−85	−239	−10.6

[a] Determined at 270 nm. Data without parentheses are measured in 1 M NaCl containing 100 mM $MgCl_2$ and 60 mM sodium cacodylate (pH = 7.0) with 10 μM oligonucleotide concentration. Data in parentheses are measured in 0.1 M NaCl, 10 mM $MgCl_2$ and 10 mM sodium cacodylate (pH = 7.0) with 10 μM oligonucleotide concentration. [b] 1 cal = 4.184 J.

(4×10^4 Pa) using the following solvent systems: (A) CH_2Cl_2–MeOH (9 : 1 v/v), (B) petroleum spirit (boiling range 40–60 °C)–acetone (1 : 1, v/v). Samples were collected with an UltroRac II fractions collector (LKB Instruments, Sweden).

Oligonucleotides. Oligonucleotide synthesis was performed on a 380-B DNA synthesizer (Applied Biosystems, Weiterstadt, Germany) using a standard protocol. The oligonucleotides were purified by oligonucleotide purification cartridges.[25] The enzymic hydrolysis of the oligomers was performed as described in ref. 39. Quantification of the constituents was made on the basis of the peak areas, which were divided by the extinction coefficients of the nucleoside (ε_{260}-values: dA 15 400, dC 7300, dG 11 400, dT 8800, c^{7}z^{8}A$_d$ 9500,[5] I^{7}c^{7}z^{8}A$_d$ 7200, Br^{7}c^{7}z^{8}A$_d$ 4600, Hxy^{7}c^{7}z^{8}A$_d$ 7900, Phy^{7}c^{7}z^{8}Ad$_d$ 11 900 dm^3 mol^{-1} cm^{-1}). Snake venom phosphodiesterase (EC 3.1.15.1, *Crotalus durissus*) and alkaline phosphatase (EC 3.1.3.1, *E. coli*) were generous gifts of Roche Diagnostics, Germany. MALDI-TOF mass spectra were provided by Dr J. Gross (University of Heidelberg, Germany). RP-18 HPLC: 250 × 4 mm RP-18 column; Merck-Hitachi HPLC; gradient of 0.1 M (Et_3NH)OAc (pH 7.0)/MeCN 95 : 5 (A) and MeCN (B); gradient *I*: 50 min 0–50% B in A, flow rate 1 cm^3 min^{-1}.

Determination of T_m-values and of thermodynamic data. Absorbance *vs.* temperature profiles were measured on a Cary-1/1E UV/VIS spectrophotometer (Varian, Australia) equipped with a Cary thermoelectrical controller. The T_m-values were measured in the reference cell with a Pt-100 resistor and the thermodynamic data (ΔH, ΔS, $\Delta G°$) were calculated using the program "MeltWin 3.0".[26] CD spectra were recorded with a JASCO-600 (JASCO, Japan) spectropolarimeter with thermostatically (Lauda-RCS-6 bath) controlled 1 cm cuvettes.

Chemical synthesis

4-Amino-1-(2-deoxy-β-D-*erythro*-pentofuranosyl)-3-(hex-1-ynyl)-1*H*-pyrazolo[3,4-*d*]pyrimidine 1d. *Method 1.* A suspension of 4-amino-1-(2-deoxy-β-D-*erythro*-pentofuranosyl)-3-iodo-1*H*-pyrazolo[3,4-*d*]pyrimidine[8] **1c** (200 mg, 0.53 mmol) and CuI (20.2 mg, 0.106 mmol) in anhydrous DMF (3 cm^3) was treated with hex-1-yne (10 equiv.), anhydrous Et_3N (108 mg, 1.06 mmol) and $Pd(PPh_3)_4$ (62 mg, 0.054 mmol). The mixture was stirred under Ar at rt for 5 h. The mixture was diluted with MeOH–CH_2Cl_2 (10 cm^3; 1 : 1) and Dowex 1X8 (100–200 mesh; 500 mg, HCO_3^- form) was introduced. After being stirred for 45 min the mixture was filtered, and the resin washed twice with MeOH–CH_2Cl_2 (20 cm^3; 1 : 1). The combined filtrates were evaporated and the residue was subjected to FC (column 15 × 3 cm) using CH_2Cl_2 with an increasing amount of MeOH (5–10%, v/v). The main zone afforded the *nucleoside derivative* **1d** upon evaporation as a foam (102 mg, 58%).

Method 2. A suspension of bromide **1b**[8] (200 mg, 0.53 mmol) and CuI (20.2 mg, 0.106 mmol) in anhydrous DMF (3 cm^3) was treated with hex-1-yne (10 equiv.), anhydrous Et_3N (108 mg, 1.06 mmol) and $Pd(PPh_3)_4$ (62 mg, 0.054 mmol) as described above except that the reaction temperature was 45 °C. Reaction time was 48 h; product **1d** was obtained as a foam (93 mg, 53%) (Found: C, 57.9; H, 6.4; N, 21.2. $C_{16}H_{21}N_5O_3$ requires C, 57.99; H, 6.39; N, 21.13%); R_f (A) 0.50; λ_{max}(MeOH)/nm 248 (ε/dm^3 mol^{-1} cm^{-1} 9600) and 286 (9600); λ_{max}(water)/nm 230 (ε/dm^3 mol^{-1} cm^{-1} 13 900), 248 (16 400) and 278 (15 100); δ_H[250 MHz; $(CD_3)_2SO$] 0.92 (3 H, t, *J* 7.3, CH_3), 1.43 (2 H, sextet, *J* 7.3, CH_2CH_3), 1.63 (2 H, quintet, *J* 7.1, $CH_2CH_2CH_3$), 2.24 (1 H, m, 2′-H$_\alpha$), 2.52 (2 H, t, *J* 7.1, $CH_2C{\equiv}C$), 2.73 (1 H, m, 2′-H$_\beta$), 3.45 (2 H, m, 5′-H$_{\alpha,\beta}$), 3.80 (1 H, m, 4′-H), 4.41 (1 H, m, 3′-H), 4.76 (1 H, t, *J* 5.6, 5′-OH), 5.24 (1 H, d, *J* 4.5, 3′-OH), 6.52 (1 H, 't', *J* 6.4, 1′-H), 6.64 and 8.04 (2 H, 2 br s, NH_2) and 8.24 (1 H, s, 6-H).

3-Bromo-1-(2-deoxy-β-D-*erythro*-pentofuranosyl)-4-{[(dimethylamino)methylidene]amino}-1*H*-pyrazolo[3,4-*d*]pyrimidine 3a. A solution of 3-bromo-1-(2-deoxy-β-D-*erythro*-pentofuranosyl)-1*H*-pyrazolo[3,4-*d*]pyrimidine[8] **1b** (330 mg, 1 mmol) in methanol (20 cm^3) was stirred with *N*,*N*-dimethylformamide

dimethyl acetal (2.0 g, 16.8 mmol) for 2 h at 40 °C. After evaporation, the residue was applied to FC [column 12 × 3 cm, solvent (A)]. The title compound **3a** was isolated as a foam (320 mg, 83%) (Found: C, 40.2; H, 4.6; N, 20.9. $C_{13}H_{17}BrN_6O_3$ requires C, 40.53; H, 4.45; N, 21.82%); R_f (A) 0.52; λ_{max}(MeOH)/nm 236 (ε/dm^3 mol^{-1} cm^{-1} 6200), 260 (4900), 301 (7100) and 305 (7000); δ_H[250 MHz; $(CD_3)_2SO$] 2.26 (1 H, m, 2′-H$_\alpha$), 2.78 (1 H, m, 2′-H$_\beta$), 3.21 and 3.23 (6 H, 2 s, Me_2N), 3.45 (2 H, m, 5′-H$_{\alpha,\beta}$), 3.80 (1 H, m, 4′-H), 4.40 (1 H, m, 3′-H), 4.75 (1 H, br, 5′-OH), 5.27 (1 H, br, 3′-OH), 6.55 (1 H, 't', *J* 6.4, 1′-H), 8.44 (1 H, s, 6-H) and 8.94 (1 H, s, N=CH).

1-(2-Deoxy-β-D-*erythro*-pentofuranosyl)-4-{[(dimethylamino)-methylidene]amino}-3-iodo-1*H*-pyrazolo[3,4-*d*]pyrimidine 3b. Compound **3b** was prepared from 1-(2-deoxy-β-D-*erythro*-pentofuranosyl)-3-iodo-1*H*-pyrazolo[3,4-*d*]pyrimidine[8] **1c** (377 mg, 1 mmol) and *N*,*N*-dimethylformamide dimethyl acetal (2.0 g, 16.8 mmol) as described for analogue **3a**. After FC [column 12 × 3 cm, solvent (A)] *title compound* **3b** was obtained as a foam (367 mg, 85%) (Found: C, 36.4; H, 4.2; N, 19.4. $C_{13}H_{17}IN_6O_3$ requires C, 36.13; H, 3.96; N, 19.44%); R_f(A) 0.53; λ_{max}(MeOH)/nm 262 (ε/dm^3 mol^{-1} cm^{-1} 7100) and 321 (16 900); δ_H[250 MHz; $(CD_3)_2SO$] 2.24 (1 H, m, 2′-H$_\alpha$), 2.80 (1 H, m, 2′-H$_\beta$), 3.23 and 3.26 (6 H, 2 s, Me_2N), 3.45 (2 H, m, 5′-H$_{\alpha,\beta}$), 3.81 (1 H, m, 4′-H), 4.40 (1 H, m, 3′-H), 4.75 (1 H, t, *J* 5.7, 5′-OH), 5.25 (1 H, d, *J* 4.5, 3′-OH), 6.52 (1 H, 't', *J* 6.5, 1′-H), 8.42 (1 H, s, 6-H) and 8.95 (1 H, s, N=CH).

1-(2-Deoxy-β-D-*erythro*-pentofuranosyl)-4-{[(dimethylamino)-methylidene]amino}-3-(hex-1-ynyl)-1*H*-pyrazolo[3,4-*d*]pyrimidine 3c. Compound **3c** was prepared from compound **1d** (330 mg, 1 mmol) and *N*,*N*-dimethylformamide dimethyl acetal (2.0 g, 16.8 mmol) as described for analogue **3a**. After FC [column 12 × 3 cm, solvent (A)] *title compound* **3c** was obtained as a foam (310 mg, 80%) (Found: C, 59.3; H, 6.9; N, 21.4. $C_{19}H_{26}N_6O_3$ requires C, 59.05; H, 6.78; N, 21.75%); R_f(A) 0.55; λ_{max}(MeOH)/nm 288 (ε/dm^3 mol^{-1} cm^{-1} 11 400), 297 (10 800) and 320 (11 600); δ_H[500 MHz; $(CD_3)_2SO$] 0.92 (3 H, t, *J* 7.2, CH_3), 1.47 (2 H, sextet, *J* 7.2, CH_2CH_3), 1.57 (2 H, quintet, *J* 7.3, $CH_2CH_2CH_3$), 2.26 (1 H, m, 2′-H$_\alpha$), 2.51 (2 H, CH_2, superimposed by DMSO), 2.82 (1 H, m, 2′-H$_\beta$), 3.21 and 3.24 (6 H, 2 s, Me_2N), 3.46 (2 H, m, 5′-H$_{\alpha,\beta}$), 3.84 (1 H, m, 4′-H), 4.45 (1 H, m, 3′-H), 4.75 (1 H, t, *J* 5.6, 5′-OH), 5.26 (1 H, d, *J* 4.3, 3′-OH), 6.59 (1 H, 't', *J* 6.3, 1′-H), 8.44 (1 H, s, 6-H) and 8.91 (1 H, s, N=CH).

1-(2-Deoxy-β-D-*erythro*-pentofuranosyl)-4-{[(dimethylamino)-methylidene]amino}-3-(2-phenylethynyl)-1*H*-pyrazolo[3,4-*d*]-pyrimidine 3d. Compound **3d** was prepared from 1-(2-deoxy-β-D-*erythro*-pentofuranosyl)-3-(2-phenylethynyl)-1*H*-pyrazolo-[3,4-*d*]pyrimidine[8] **1e** (350 mg, 1 mmol) and *N*,*N*-dimethylformamide dimethyl acetal (2.0 g, 16.8 mmol) as described for analogue **3a**. After FC [column 12 × 3 cm, solvent (A)] *title compound* **3d** was obtained as a foam (322 mg, 79%) (Found: C, 61.9; H, 5.4; N, 20.55. $C_{21}H_{22}N_6O_3$ requires C, 62.06; H, 5.46; N, 20.68%); R_f(A) 0.56; λ_{max}(MeOH)/nm 249 (ε/dm^3 mol^{-1} cm^{-1} 20 000), 270 (17 500) and 312 (24 900); δ_H[500 MHz; $(CD_3)_2SO$] 2.31 (1 H, m, 2′-H$_\alpha$), 2.87 (1 H, m, 2′-H$_\beta$), 3.20 and 3.23 (6 H, 2 s, Me_2N), 3.49 (2 H, m, 5′-H$_{\alpha,\beta}$), 3.87 (1 H, m, 4′-H), 4.48 (1 H, m, 3′-H), 4.78 (1 H, t, *J* 5.7, 5′-OH), 5.30 (1 H, d, *J* 4.5, 3′-OH), 6.65 (1 H, 't', *J* 6.4, 1′-H), 7.48 (3 H, m, ArH), 7.63 (2 H, m, ArH), 8.49 (1 H, s, 6-H) and 8.96 (1 H, s, N=CH).

4-Benzamido-1-(2-deoxy-β-D-*erythro*-pentofuranosyl)-3-iodo-1*H*-pyrazolo[3,4-*d*]pyrimidine 4a. Compound **1c**[8] (380 mg, 1.0 mmol) was dissolved in pyridine (5 cm^3), and the solution was treated with Me_3SiCl (1.3 cm^3, 10.2 mmol) while being stirred at rt. After 30 min, benzoyl chloride (650 mm^3, 5.0 mmol) was added and the mixture was kept at rt for 2 h before being cooled to 0 °C, diluted with water (2 cm^3), and, after 10 min, treated with 12% aq. NH_3 (2 cm^3; 1 h; rt). The solution was evaporated and the residue was applied to FC [column 15 × 3 cm, solvent (A)]. Crystallization from MeOH afforded the *title benzamide* as needles (259 mg, 54%), mp 218–219 °C (from MeOH, decomp.) (Found: C, 42.3; H, 3.4; N, 14.6. $C_{17}H_{16}IN_5O_4$ requires C, 42.43; H, 3.35; N, 14.55%); R_f(A) 0.55; λ_{max}(MeOH)/nm 243 (ε/dm^3 mol^{-1} cm^{-1} 8300), 263 (8200) and 280 (8500); δ_H[500 MHz; $(CD_3)_2SO$] 2.35 (1 H, m, 2′-H$_\alpha$), 2.84 (1 H, m, 2′-H$_\beta$), 3.46 (2 H, m, 5′-H$_{\alpha,\beta}$), 3.87 (1 H, m, 4′-H), 4.47 (1 H, m, 3′-H), 4.72 (1 H, t, *J* 5.6, 5′-OH), 5.31 (1 H, d, *J* 4.5, 3′-OH), 6.65 (1 H, 't', *J* 6.3, 1′-H), 7.60 (3 H, m, ArH), 8.15 (2 H, m, ArH), 8.68 (1 H, s, 6-H) and 11.30 (1 H, s, NH).

1-(2-Deoxy-β-D-*erythro*-pentofuranosyl)-3-iodo-4-isobutyramido-1*H*-pyrazolo[3,4-*d*]pyrimidine 4b. Compound **1c**[8] (380 mg, 1 mmol) in pyridine (5 cm^3) was treated with Me_3SiCl (1.3 cm^3, 10.2 mmol) and isobutyryl chloride (530 mg, 5.0 mmol) as described for analogue **4a** except that the treatment with 6% aq. NH_3 (2 cm^3; rt) took 15 min. Evaporation, FC [column 15 × 3 cm, solvent (A)] and crystallization (MeOH) afforded the *title isobutyramide* as needles (213 mg, 48%), mp 202–204 °C (from MeOH, decomp.) (Found: C, 37.4; H, 3.9; N, 15.7. $C_{14}H_{18}IN_5O_4$ requires C, 37.60; H, 4.06; N, 15.66%); R_f(A) 0.55; λ_{max}(MeOH)/nm 232 (ε/dm^3 mol^{-1} cm^{-1} 13 400), 263 (9100) and 283 (10 900); δ_H[500 MHz; $(CD_3)_2SO$] 1.22 and 1.23 (6 H, 2 s, 2 × CH_3), 2.33 (1 H, m, 2′-H$_\alpha$), 2.86 (2 H, m, 2′-H$_\beta$ and CH), 3.45 (2 H, m, 5′-H$_{\alpha,\beta}$), 3.84 (1 H, m, 4′-H), 4.46 (1 H, m, 3′-H), 4.72 (1 H, t, *J* 5.4, 5′-OH), 5.30 (1 H, d, *J* 4.1, 3′-OH), 6.65 (1 H, 't', *J* 6.3, 1′-H), 8.79 (1 H, s, 6-H) and 10.65 (1 H, s, NH).

3-Bromo-1-[2-deoxy-5-*O*-(4,4′-dimethoxytriphenylmethyl)-β-D-*erythro*-pentofuranosyl]-4-{[(dimethylamino)methylidene]-amino}-1*H*-pyrazolo[3,4-*d*]pyrimidine 5a. To a solution of **3a** (300 mg, 0.78 mmol) in dry pyridine (2 cm^3) was added 4,4′-dimethoxytriphenylmethyl chloride (290 mg, 0.86 mmol). After being stirred at 50 °C for 1 h the mixture was poured into ice-cold 3% aq. $NaHCO_3$ (10 cm^3) and extracted quickly with CH_2Cl_2 (2 × 100 cm^3). The combined organic layers were dried over Na_2SO_4, filtered and evaporated. The residue was applied to FC [column 15 × 3 cm, solvent (A)]. The *title compound* **5a** was isolated as a foam (375 mg, 70%) (Found: C, 59.5; H, 5.3; N, 12.1. $C_{34}H_{35}BrN_6O_5$ requires C, 59.39; H, 5.13; N, 12.22%); R_f(A) 0.62; λ_{max}(MeOH)/nm 230 (ε/dm^3 mol^{-1} cm^{-1} 20 700), 262 (7100), 282 (9200) and 321 (5200); δ_H[250 MHz; $(CD_3)_2SO$] 2.31 (1 H, m, 2′-H$_\alpha$), 2.82 (1 H, m, 2′-H$_\beta$), 3.00 (2 H, m, 5′-H$_{\alpha,\beta}$), 3.21 and 3.23 (6 H, 2 s, Me_2N), 3.68 and 3.69 (6 H, 2 s, 2 × MeO), 3.93 (1 H, m, 4′-H), 4.51 (1 H, m, 3′-H), 5.30 (1 H, d, *J* 4.8, 3′-OH), 6.58 (1 H, 't', *J* 6.5, 1′-H), 6.73 (4 H, m, ArH), 7.14–7.31 (9 H, m, ArH), 8.47 (1 H, s, 6-H) and 8.94 (1 H, s, N=CH).

1-[2-Deoxy-5-*O*-(4,4′-dimethoxytriphenylmethyl)-β-D-*erythro*-pentofuranosyl]-4-{[(dimethylamino)methylidene]-amino}-3-iodo-1*H*-pyrazolo[3,4-*d*]pyrimidine 5b. As described for analogue **5a**, compound **3b** (300 mg, 0.69 mmol) was treated with 4,4′-dimethoxytriphenylmethyl chloride (280 mg, 0.83 mmol). FC [column 15 × 3 cm, solvent (A)] furnished *title compound* **5b** as a foam (365 mg, 72%) (Found: C, 55.5; H, 4.6; N, 11.3. $C_{34}H_{35}IN_6O_5$ requires C, 55.56; H, 4.80; N, 11.44%); R_f(A) 0.63; λ_{max}(MeOH)/nm 230 (ε/dm^3 mol^{-1} cm^{-1} 25 200), 284 (8900) and 322 (18 700); δ_H[500 MHz; $(CD_3)_2SO$] 2.30 (1 H, m, 2′-H$_\alpha$), 2.84 (1 H, m, 2′-H$_\beta$), 3.07 (2 H, m, 5′-H$_{\alpha,\beta}$), 3.26 and 3.28 (6 H, 2 s, Me_2N), 3.71 and 3.72 (6 H, 2 s, 2 × MeO), 3.95 (1 H, m, 4′-H), 4.52 (1 H, m, 3′-H), 5.30 (1 H, d, *J* 3.9, 3′-OH), 6.58 (1 H, 't', *J* 5.8, 1′-H), 6.78 (4 H, m, ArH), 7.13–7.37 (9 H, m, ArH), 8.47 (1 H, s, 6-H) and 8.98 (1 H, s, N=CH).

1-[2-Deoxy-5-*O*-(4,4′-dimethoxytriphenylmethyl)-β-D-*erythro*-pentofuranosyl]-4-{[(dimethylamino)methylidene]-amino}-3-(hex-1-ynyl)-1*H*-pyrazolo[3,4-*d*]pyrimidine 5c. As described for analogue **5a**, compound **3c** (300 mg, 0.78 mmol) was treated with 4,4′-dimethoxytriphenylmethyl chloride (300

mg, 0.89 mmol). FC [column 15 × 3 cm, solvent (A)] furnished *title compound* **5c** as a foam (322 mg, 60%) (Found: C, 69.9; H, 6.7; N, 12.6. $C_{40}H_{44}N_6O_5$ requires C, 69.75; H, 6.44; N, 12.20%); R_f(A) 0.67; λ_{max}(MeOH)/nm 274 (ε/dm^3 mol^{-1} cm^{-1} 12 800), 282 (12 800) and 320 (18 200); δ_H[250 MHz; $(CD_3)_2SO$] 0.88 (3 H, t, *J* 7.2, CH_3), 1.43 (2 H, sextet, *J* 7.2, CH_2CH_3), 1.54 (2 H, quintet, *J* 7.2, $CH_2CH_2CH_3$), 2.31 (1 H, m, 2′-H$_\alpha$), 2.50 (2 H, CH_2, superimposed by DMSO), 2.82 (1 H, m, 2′-H$_\beta$), 3.03 (2 H, m, 5′-H$_{\alpha,\beta}$), 3.19 and 3.22 (6 H, 2 s, Me_2N), 3.69 and 3.70 (6 H, 2 s, 2 × MeO), 3.92 (1 H, m, 4′-H), 4.53 (1 H, m, 3′-H), 5.31 (1 H, d, *J* 4.9, 3′-OH), 6.60 (1 H, 't', *J* 6.5, 1′-H), 6.73 (4 H, m, ArH), 7.14–7.32 (9 H, m, ArH), 8.46 (1 H, s, 6-H) and 8.90 (1 H, s, N=CH).

1-[2-Deoxy-5-*O*-(4,4′-dimethoxytriphenylmethyl)-β-D-*erythro*-pentofuranosyl]-4-{[(dimethylamino)methylidene]-amino}-3-(2-phenylethynyl)-1*H*-pyrazolo[3,4-*d*]pyrimidine 5d. As described for analogue **5a**, compound **3d** (300 mg, 0.74 mmol) was treated with 4,4′-dimethoxytriphenylmethyl chloride (300 mg, 0.89 mmol). FC [column 15 × 3 cm, solvent (A)] furnished *title compound* **5d** as a foam (356 mg, 68%) (Found: C, 71.2; H, 6.0; N, 11.8. $C_{42}H_{40}N_6O_5$ requires C, 71.17; H, 5.69; N, 11.86%); R_f(A) 0.67; λ_{max}(MeOH)/nm 270 (ε/dm^3 mol^{-1} cm^{-1} 18 900) and 313 (23 700); δ_H[250 MHz; $(CD_3)_2SO$] 2.30 (1 H, m, 2′-H$_\alpha$), 2.89 (1 H, m, 2′-H$_\beta$), 3.08 (2 H, m, 5′-H$_{\alpha,\beta}$), 3.17 and 3.20 (6 H, 2 s, Me_2N), 3.62 and 3.64 (6 H, 2 s, 2 × MeO), 3.93 (1 H, m, 4′-H), 4.39 (1 H, m, 3′-H), 5.34 (1 H, d, *J* 4.3, 3′-OH), 6.69–6.76 (5 H, m, 1′-H and ArH), 7.15–7.37 (9 H, m, ArH), 7.46 (3 H, m, ArH), 7.58 (2 H, m, ArH), 8.51 (1 H, s, 6-H) and 8.94 (1 H, s, N=CH).

3-Bromo-1-[2-deoxy-5-*O*-(4,4′-dimethoxytriphenylmethyl)-β-D-*erythro*-pentofuranosyl]-4-{[(dimethylamino)methylidene]-amino}-1*H*-pyrazolo[3,4-*d*]pyrimidine 3′-[(2-cyanoethyl) *N*,*N*-diisopropylphosphoramidite] 2a. To a stirred solution of dry nucleoside **5a** (300 mg, 0.44 mmol) and anhydrous *N*,*N*-diisopropylethylamine (DIPEA) (170 mg, 1.32 mmol) in dry THF (2 cm^3) was added chloro(2-cyanoethoxy)(*N*,*N*-diisopropylamino)phosphine (137 mg, 0.58 mmol) under Ar. The reaction mixture was stirred for 30 min and was then filtered. The filtrate was diluted with ethyl acetate (80 cm^3) and extracted twice successively with ice-cold aq. 3% $NaHCO_3$ (2 × 10 cm^3) and water (2 × 10 cm^3). The organic phase was dried over Na_2SO_4, filtered and evaporated to dryness. The residue was applied to FC [column 12 × 2 cm, solvent (B)]. The *title compound* **2a** was isolated as an oil (266 mg, 68%). R_f(B) 0.4 and 0.5; δ_P[101 MHz; $CDCl_3$] 148.9 and 149.0.

1-[2-Deoxy-5-*O*-(4,4′-dimethoxytriphenylmethyl)-β-D-*erythro*-pentofuranosyl]-4-{[(dimethylamino)methylidene]-amino}-3-iodo-1*H*-pyrazolo[3,4-*d*]pyrimidine 3′-[(2-cyanoethyl) *N*,*N*-diisopropylphosphoramidite] 2b. Compound **5b** (300 mg, 0.41 mmol) was treated with anhydrous DIPEA (160 mg, 1.23 mmol) and chloro(2-cyanoethoxy)(*N*,*N*-diisopropylamino)-phosphine (120 mg, 0.51 mmol) as described for analogue **2a**. FC [column 12 × 2 cm, solvent (B)] furnished *title compound* **2b** as a foam (250 mg, 65%). R_f(B) 0.4 and 0.5; δ_P[101 MHz; $CDCl_3$] 148.9 and 149.0.

1-[2-Deoxy-5-*O*-(4,4′-dimethoxytriphenylmethyl)-β-D-*erythro*-pentofuranosyl]-4-{[(dimethylamino)methylidene]-amino}-3-(hex-1-ynyl)-1*H*-pyrazolo[3,4-*d*]pyrimidine 3′-[(2-cyanoethyl) *N*,*N*-diisopropylphosphoramidite] 2c. Compound **5c** (300 mg, 0.44 mmol) was treated with anhydrous DIPEA (170 mg, 1.32 mmol) and chloro(2-cyanoethoxy)(*N*,*N*-diisopropylamino)phosphine (137 mg, 0.58 mmol) as described for analogue **2a**. FC [column 12 × 2 cm, solvent (B)] furnished *title compound* **2c** as a foam (250 mg, 64%). R_f(B) 0.4 and 0.5; δ_P[101 MHz; $CDCl_3$] 148.9 and 149.0.

1-[2-Deoxy-5-*O*-(4,4′-dimethoxytriphenylmethyl)-β-D-*erythro*-pentofuranosyl]-4-{[(dimethylamino)methylidene]-amino}-3-(2-phenylethynyl)-1*H*-pyrazolo[3,4-*d*]pyrimidine 3′-[(2-cyanoethyl) *N*,*N*-diisopropylphosphoramidite] 2d. Compound **5d** (300 mg, 0.42 mmol) was treated with anhydrous DIPEA (163 mg, 1.26 mmol) and chloro(2-cyanoethoxy)(*N*,*N*-diisopropylamino)phosphine (118 mg, 0.50 mmol) as described for analogue **2a**. The *title compound* **2d** was isolated after FC [column 12 × 2 cm, solvent (B)] as a foam (267 mg, 70%). R_f(B) 0.4 and 0.5; δ_P[101 MHz; $CDCl_3$] 148.9 and 149.1.

Acknowledgements

Financial support by the 'Bundesministerium für Bildung, Wissenschaft, Forschung und Technologie (BMFT)' is gratefully acknowledged. We also thank Dr Jürgen Gross, University of Heidelberg for the MALDI-TOF mass spectra.

References

1 F. Seela and M. Zulauf, *Chem. Eur. J.*, 1998, **4**, 1781.
2 F. Seela and H. Thomas, *Helv. Chim. Acta*, 1995, **78**, 94.
3 N. Ramzaeva and F. Seela, *Helv. Chim. Acta*, 1996, **79**, 1549.
4 N. Ramzaeva, C. Mittelbach and F. Seela, *Helv. Chim. Acta*, 1997, **80**, 1809.
5 F. Seela and H. Steker, *Helv. Chim. Acta*, 1985, **68**, 563.
6 F. Seela and H. Steker, *Helv. Chim. Acta*, 1986, **69**, 1602.
7 F. Seela, M. Zulauf and G. Becher, *Nucleosides, Nucleotides*, 1997, **16**, 305.
8 F. Seela and M. Zulauf, *J. Chem. Soc.*, *Perkin Trans. 1*, 1998, 3233.
9 F. Seela and G. Becher, *Synthesis*, 1998, 207.
10 N. Sugimoto and T. Sato, *Jap. Pat.* 61 109 797, 1986 (*Chem. Abstr.*, 1987, **106**, 214304h).
11 C. R. Petrie, A. D. Adams, M. Stamm, J. van Ness, S. W. Watanabe and R. B. Meyer, Jr., *Bioconjugate Chem.*, 1991, **2**, 441.
12 F. Seela and K. Kaiser, *Nucleic Acids Res.*, 1986, **14**, 1825.
13 F. Seela and K. Kaiser, *Helv. Chim. Acta*, 1988, **71**, 1813.
14 F. Seela and H. Driller, *Nucleic Acids Res.*, 1989, **17**, 901.
15 F. Seela and H. Driller, *Helv. Chim. Acta*, 1988, **71**, 1191.
16 F. Seela, H. Rosemeyer, H. Driller, K. Kaiser and H. Steker, *Nucleosides, Nucleotides*, 1989, **8**, 789.
17 F. Seela, M. Zulauf and N. Ramzaeva, *Nucleosides, Nucleotides*, 1997, **16**, 963.
18 F. Seela and G. Becher, *Chem. Commun.*, 1998, 2017.
19 F. Seela, M. Zulauf and G. Becher, *Nucleosides, Nucleotides*, 1999, in the press.
20 F. Seela, H. Berg and H. Rosemeyer, *Biochemistry*, 1989, **28**, 6193.
21 S. Sprang, R. Scheller, D. Rohrer and M. Sundaralingam, *J. Am. Chem. Soc.*, 1978, **100**, 2867.
22 P. Prusiner, T. Brennan and M. Sundaralingam, *Biochemistry*, 1973, **12**, 1196.
23 F. Seela, M. Zulauf, G. Kastner and H. Reuter, unpublished.
24 G. S. Ti, B. L. Gaffney and R. A. Jones, *J. Am. Chem. Soc.*, 1982, **104**, 1316.
25 User Manual for Oligonucleotide Purification Cartridges, Applied Biosystems.
26 J. A. McDowell and D. H. Turner, *Biochemistry*, 1996, **35**, 14077.
27 R. E. Dickerson and H. R. Drew, *J. Mol. Biol.*, 1981, **149**, 761.
28 F. Seela and A. Kehne, *Biochemistry*, 1987, **26**, 2232.
29 L. A. Marky, K. S. Blumenfeld, S. Kozlowski and K. J. Breslauer, *Biopolymers*, 1983, **22**, 1247.
30 E. T. Kool, *Chem. Rev.*, 1997, **97**, 1473.
31 E. A. Lesnik and S. M. Freier, *Biochemistry*, 1995, **34**, 10807.
32 D. Graham, J. A. Parkinson and T. Brown, *J. Chem. Soc.*, *Perkin Trans. 1*, 1998, 1131.
33 E. Dias, J. L. Battiste and J. R. Williamson, *J. Am. Chem. Soc.*, 1994, **116**, 4479.
34 R. G. Eason, D. M. Burkhardt, S. J. Phillips, D. P. Smith and S. S. David, *Nucleic Acids Res.*, 1996, **24**, 890.
35 F. Seela and Y. Chen, *Chem. Commun.*, 1996, 2263.
36 F. Seela, M. Zulauf, H. Rosemeyer and H. Reuter, *J. Chem. Soc.*, *Perkin Trans. 2*, 1996, 2373.
37 W. K. Olson and R. D. Dasika, *J. Am. Chem. Soc.*, 1976, **98**, 5371.
38 W. K. Olson, *Proc. Natl. Acad. Sci. USA*, 1977, **74**, 1775.
39 F. Seela and S. Lampe, *Helv. Chim. Acta*, 1991, **74**, 1790.

Paper 8/08769E